Biosensors and Bioelectronics 60 (2014) 305–310

Contents lists available at ScienceDirect

Biosensors and Bioelectronics

journal homepage: www.elsevier.com/locate/bios

Towards sensitive label-free immunosensing by means of turn-around point long period fiber gratings

F. Chiavaioli [a], P. Biswas [b,*], C. Trono [a,**], S. Bandyopadhyay [b], A. Giannetti [a], S. Tombelli [a], N. Basumallick [b], K. Dasgupta [b], F. Baldini [a]

[a] Institute of Applied Physics "Nello Carrara", National Research Council, Via Madonna del Piano 10, 50019 Sesto Fiorentino (FI), Italy
[b] Central Glass and Ceramic Research Institute, Council of Scientific and Industrial Research, 196 Raja S C Mullick Road, Kolkata 700032, India

ARTICLE INFO

Article history:
Received 30 January 2014
Received in revised form
11 April 2014
Accepted 22 April 2014
Available online 2 May 2014

Keywords:
Optical fiber biosensor
Long period grating
Turn-around point
Immunosensor
Label-free
Serum

ABSTRACT

Long period fiber gratings have been effectively used in the field of biochemical sensing since a few years. Compared to other well-known label-free optical approaches, long period gratings (LPGs) take advantage of the typical peculiarity of optical fibers. Coupling the propagating core mode with a high-order cladding mode near its turn-around point (TAP) was the strategy adopted to achieve good performances without additional coatings, except for the sensing and selective biolayer deposited on the fiber. Both the modeling and manufacturing of TAP LPGs were discussed. After the functionalization of the fiber surface with the deposition of a Eudragit L100 copolymer layer followed by immunoglobulin G (IgG) covalent immobilization, an IgG/anti-IgG bioassay was implemented along the grating region and the kinetics of antibody/antigen interaction was analyzed. A quantitative comparison between a TAP LPG and a non-TAP LPG was carried out to highlight the improvement of the proposed immunosensor. The real effectiveness and feasibility of an LPG-based biosensor were demonstrated by using a complex matrix consisting of human serum, which also confirmed the specificity of the assay, and a limit of detection of 70 μg L^{-1} (460 pM) was achieved.

1. Introduction

Label-free optical biosensors are increasingly finding applications in fast, reliable and in situ measurements in the field of chemical, biochemical and biomedical sensing and nowadays are certainly among the most fascinating and groundbreaking fields of research (Wang and Wolfbeis, 2013). Based on the measurement of refractive index (RI) changes, induced by a chemical and/or a biochemical interaction with a sensing layer deposited on a suitable substrate, they are able not only to allow the quantitative measurement of the investigated analyte, but also to provide the unique chance to analyze the dynamic interactions. Among all the optical approaches providing a sensitive and accurate measurement of RI, those based on surface plasmon resonance (SPR) are the most widespread ones (Homola, 2008; Estevez et al., 2014; Voisin et al., 2014), with values of resolution down to 10^{-7} RI units (RIU) (Piliarik and Homola, 2009). Other interesting and competitive approaches are based on interferometric configurations, implemented on optical fibers and planar waveguides, and on resonating structures (Fan et al., 2008; Kindt and Bailey, 2013).

Optical fiber long period gratings (LPGs) constitute a novel promising class of label-free optical biosensors (Eftimov, 2010; Baldini et al., 2012). An LPG is characterized by a series of periodic RI changes of the order of hundreds of μm in the core of a single-mode optical fiber, capable to create a modulation pattern that runs along the fiber axis; this property provides the condition for a wavelength-dependent coupling between the propagating core mode and the cladding modes. Consequently, one or more attenuation bands characterize the transmission spectrum of an LPG, with the minimum of each band representing the coupling with a selective cladding mode that occurs at a well-defined wavelength, the resonance wavelength λ_{res} (Erdogan, 1997). Compared to the other well-known optical approaches, LPGs exploit the peculiarities of optical fibers, such as compactness, lightweight, intrinsic miniaturization, high compatibility with optoelectronic devices used in the telecommunication windows (i.e. 1.3 μm and 1.5 μm), as well as multiplexing and remote measurement capabilities since the signal is spectrally modulated. Therefore, LPG-based biosensors can become a real alternative to the more consolidated label-free approaches when the advantages of the use of optical fibers can play a fundamental role (e.g. in

* Corresponding author. Tel.: +913324838083.
** Corresponding author. Tel.: +390555226359.
E-mail addresses: palas@cgcri.res.in (P. Biswas), c.trono@ifac.cnr.it (C. Trono).

http://dx.doi.org/10.1016/j.bios.2014.04.042
0956-5663/

distributed sensing). The literature until now accounts for several examples of LPG-based chemical sensors and biosensors (Shevchenko et al., 2011; Chiavaioli et al., 2014; Deep et al., 2012; Korposh et al., 2012; Pilla et al., 2012a; Tripathi et al., 2012; Yang et al., 2012; Lepinay et al., 2014; Voisin et al., 2014).

When a chemical or biochemical sensing layer is deposited onto the grating region, the interaction with the investigated analyte gives rise to a modification of the RI. In this case, only a portion of the optical radiation, which comes out of the LPG, is affected, depending on both the thickness of the interaction region and the penetration depth of the evanescent field related to the coupled cladding mode (Baldini et al., 2012). One of the reasons that has prevented LPG-based biosensors from reaching competitive values of limit of detection is the lack of a reliable and effective mechanical and thermal stabilization in the measuring setup. In fact, an LPG sensor is also sensitive to strain and temperature and this dependence greatly affects the accuracy of the RI measurements. With this in mind, some examples of compensated RI measurements were proposed in the literature (Trono et al., 2011; Garg et al., 2013). Moreover, it should be noted that the best performance of these devices in terms of RI sensitivity is achieved for a surrounding RI close to the RI of fiber cladding (i.e. 1.44–1.46 RIU) (Patrick et al., 1998), far from the RI range of the aqueous samples (i.e. 1.33–1.34 RIU) which are generally used in biosensing applications. In order to overcome this problem, two different approaches were proposed. In the first approach, a thin overlayer of RI higher than the cladding RI is deposited on the fiber. By selecting a suitable value of both the RI and thickness of the overlayer, a great increase of the RI sensitivity was observed for measurements in aqueous solutions (Del Villar et al., 2005; Pilla et al., 2012b). Despite the outstanding novelty of this approach, the deposition of an overlayer makes the sensor manufacturing process longer and adds additional time-consuming chemical treatments onto the fiber. The second approach consists of coupling the propagating core mode with a high-order cladding mode near its turn-around point (TAP) (Ramachandran et al., 2002), without the application of any additional layer between the fiber and the surrounding medium. In this case, the relationship between the grating period and the resonance wavelengths, at which the coupling between the propagating core mode and the cladding modes takes place, is described by the phase-matching curves (PMCs). Typically, the slope of PMCs for higher order mode exhibits a change in sign from positive to negative and thus, for a specific grating period, the transmission spectrum of the LPG exhibits two resonant bands characterized by two resonance wavelengths. TAP is defined as the point in the PMC of a specific cladding mode of an LPG at which the two resonant bands of the same cladding mode merge into a broader resonant band. The TAP wavelength is different for each cladding mode and decreases with the increase of the mode order. It was proved that the highest RI sensitivity of LPGs is achieved around the TAP (Shu et al., 2002). Furthermore, it is possible to perform a differential measurement, i.e. the spectral difference between the minima of the two bands, which increases the total shift of λ_{res} during the RI measurements. Henceforth, the measured parameter becomes the spectral difference $\Delta\lambda_{res}$ between the λ_{res} at longer wavelengths (hereafter called red resonance wavelength λ_{RED}) and the λ_{res} at shorter wavelengths (hereafter called blue resonance wavelength λ_{BLUE}).

In the present work, a TAP LPG for sensitive label-free biosensing is proposed and fully characterized. After the functionalization of the fiber surface using Eudragit L100 copolymer, an IgG/anti-IgG immunoassay was performed in buffer and the kinetics of antibody/antigen interaction was analyzed and a quantitative comparison between the TAP LPG and a non-TAP LPG was carried out. Finally, in order to assess the real effectiveness and feasibility of an LPG-based biosensor, the calibration curve of the immunosensor was achieved, using a complex matrix such as human serum that also proved the specificity of the assay.

2. Materials and methods

2.1. Chemicals

Ethanol (EtOH), bovine serum albumin (BSA) and all the reagents for buffer preparation (phosphate-buffered saline (PBS), 40 mM, pH 7.4) were purchased from Sigma-Aldrich (Milan, Italy). Glycerol was purchased from RPE-ACS Carlo Erba Reagents (Milan, Italy). The methacrylic acid/methacrylate copolymer (Eudragit L100) was purchased from Evonik Degussa GmbH (Düsseldorf, Germany). Mouse IgG and goat anti-mouse-IgG were purchased from Zymed Laboratories, Invitrogen Immunodetection (Milan, Italy). 1-Ethyl-3-[3-dimethylaminopropyl] carbodiimide hydrochloride (EDC) and N-hydroxysuccinimide (NHS) were purchased from Pierce (Illinois, USA). A monoclonal antibody anti-PSA (prostate-specific antigen) was kindly provided by EXBIO (Praha, Czech Republic). Human serum (C Reactive Protein Free Serum) was purchased by HyTest Ltd. (Turku, Finland).

2.2. Manufacturing of the TAP LPGs

The TAP LPGs used in this experiment were inscribed in a standard single-mode fiber (SMF28e, Corning Inc.). The fiber was hydrogen loaded at a pressure of 1500 psi (10.34 MPa) and a temperature of 100 °C for 48 h in order to increase the fiber photosensitivity. A point-to-point technique was used for the manufacturing of LPGs (Hill and Meltz, 1997) by means of a KrF pulsed Excimer laser (Braggstar-500, Tuilaser, Germany) operating at a wavelength of 248 nm. LPGs with dual resonant bands were written and then the two resonance wavelengths were adjusted up to their conversion into a one broader resonant band (i.e. TAP) by reducing the diameter of the fiber cladding. The results of the theoretical modeling and of the final manufacturing of TAP LPGs are explained in Section 3.1.

2.3. The sensing layer and the bioassay protocol

The functionalization of the optical fiber in correspondence of the LPG was achieved by the deposition of a layer of Eudragit L100 consisting of approximately a 1:1 ratio of ester groups and free carboxyl functional groups (–COOH) useful for antibody immobilization. The Eudragit L100 was dissolved (0.04 w/v%) in ethanol and this solution was used for coating the fiber surface by immersion for 1 min and evaporation in air (15 min).

Once the TAP LPG was functionalized, the optical fiber was placed inside a temperature-stabilized closed flow cell with a total volume of 50 μL (Trono et al., 2011). All the steps for the implementation of the immunoassay were performed using the flow cell connected to a peristaltic pump and keeping the temperature of the flow cell at (23 ± 0.1) °C. The followed bioassay protocol was already described in a previous publication (Chiavaioli et al., 2014). The preparation of the biolayer consisted of the following steps: activation of –COOH groups by cross-linking chemistry (EDC and NHS), covalent immobilization of mouse IgG (1000 mg L^{-1} in PBS), washing with PBS for removing the un-reacted antibodies, and surface passivation with BSA (3% in PBS) in order to block the remaining activated carboxylic groups and to prevent non-specific adsorption onto the surface.

As preliminary characterization and for comparison purposes with a non-TAP LPG, the antigen binding step was performed in PBS. An anti-PSA antibody was used as negative control at a concentration of 1 mg L^{-1}. In order to validate the performance of the TAP LPG as biosensor, the assay was also performed in

human serum, a complex matrix with respect to buffer, spiked with increasing concentrations of goat anti-mouse IgG ranging from 1 μg L^{-1} up to 100 mg L^{-1}. The serum was used at a final dilution of 1:10 (v/v) in PBS.

2.4. Interrogation setup and data analysis

A broadband optical source (commercial halogen lamp) was used along with a spectrum analyzer with a spectral bandwidth of 500 nm (OSA, Anritsu MS9030A-MS9701B). In this way, it was possible to monitor the whole transmission spectrum of the TAP LPGs with both the two resonant bands (when present). The OSA is then connected to a personal computer and is controlled by means of a customized NI–CVI® program. After the acquisition of the full spectrum from 1100 nm to 1600 nm, the data analysis is performed using another NI–CVI® program that automatically calculates the minimum wavelengths by fitting the resonant band with a Lorentzian function. The acquisition time is about 20 s. In this way, it is possible to monitor in real-time any kind of kinetics of interaction that could occur between the surface and the sample under investigation. The error on the extraction of the resonance wavelength by means of the fitting procedure is lower than 1%, with a resolution of 10 pm.

3. Results and discussion

3.1. Modeling and final manufacturing of the TAP LPGs

The matrix method proposed by Anemogiannis et al. (2003) was used to model theoretically LPGs with dual resonant bands surrounded by air. A three-layer model, where the structure consists of the fiber core, the cladding and air as external medium, was used. In order to select the correct value of the grating period, the plot of phase-matching curves between the propagating core mode ($LP_{0,1}$) and few higher order cladding modes, e.g. from $LP_{0,10}$ to $LP_{0,15}$, was calculated for the fiber (SMF28e) used in this experiment and it is shown in Fig. S1.

To achieve a TAP LPG with λ_{res} in the optical telecommunication window (i.e. 1.3–1.6 μm), the grating period must be in the range 130–200 μm, with the resulting cladding mode orders of interest lying in the range 11th – 14th. On this basis, LPGs of length $L \sim 15.2$ mm with a grating period Λ of 165 μm were manufactured. Afterwards, the gratings were annealed at 150 °C for about 8 h to release the excess of hydrogen in order to stabilize the optical characteristics of the LPG. As showed in the literature (Chen et al., 2007), the PMC of each cladding mode of an LPG also depends on the thickness of the fiber cladding; therefore, it is possible to choose the coupling condition with a selected grating period Λ by means of the fine tuning of the diameter of fiber cladding d_{clad}. Fig. 1(a) shows the result of a simulation that describes the dependence of the PMC for the considered cladding mode $LP_{0,12}$ with respect to the diameter of the fiber cladding. As can be seen from Fig. 1(a), the resonant bands converge to a single one at the TAP and then vanish for a given Λ if the cladding thickness is reduced beyond a definite value. The simulated evolution of the LPG spectrum with $\Lambda = 165$ μm for decreasing thickness of d_{clad} from 125 μm up to 123.4 μm is shown in Fig. S2.

As mentioned above, it is possible to obtain two resonant bands for a fiber diameter of 125 μm as shown by means of the two black dots in Fig. 1(a), the resonance wavelengths of which coincide with the solid black line shown in Fig. 1(b). Based on these results, we slowly etched the fiber using a solution of 1% hydrofluoric acid (HF), monitoring online the spectrum until the dual resonant bands combine into one at TAP for the $LP_{0,12}$ cladding mode.

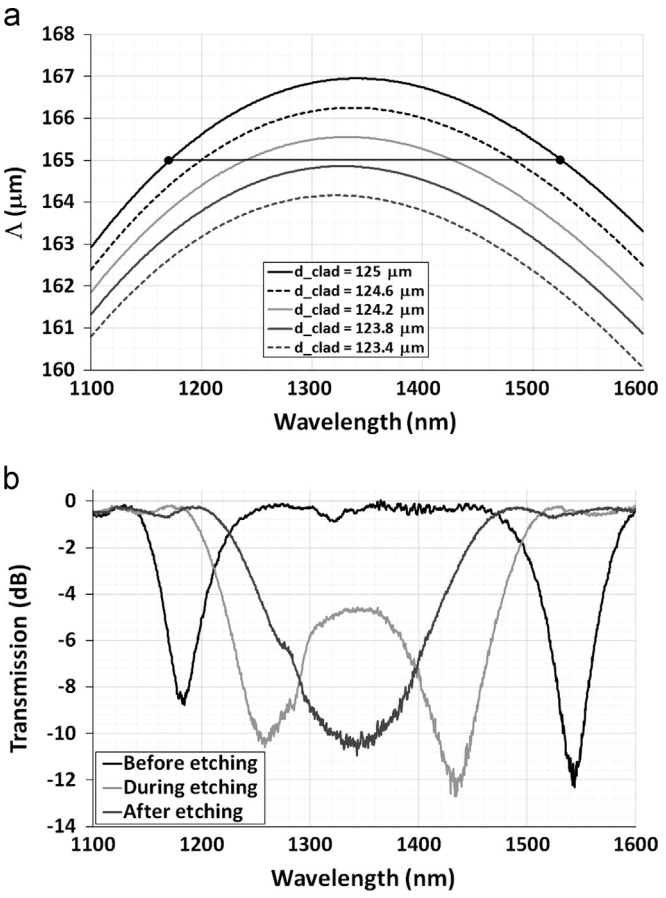

Fig. 1. (a) Phase-matching curves for $LP_{0,12}$ cladding mode as a function of the fiber diameter with a consecutive reduction of 0.4 μm, considering a grating period of 165 μm (solid black line corresponds to the non-etched fiber, whereas solid dark gray line corresponds to the closest curve to the TAP condition). (b) Spectral evolution of LPG with two resonant bands before the etching process (solid black line), during the etching with closer bands (solid light gray line), up to TAP after the etching (solid dark gray line) for the $LP_{0,12}$ cladding mode.

3.2. Characterization of the TAP LPGs

Since LPGs are sensitive not only to RI changes but also to other physical factors, i.e. fiber bending, axial strain and temperature, the characterization in terms of the above-mentioned cross-sensitivities is necessary. The fiber is placed inside the flow cell (see Section 2.3) stabilized at a selected temperature and it is fixed under a given tension at the edges of the flow cell in order to avoid both bending and axial strain (Trono et al., 2011).

Temperature characterization of the TAP LPG is detailed in Supplementary materials. The results of this characterization evidenced that the integration of an LPG in a thermo-stabilized optofluidic system is crucial when this kind of device is used as biosensor (Baldini et al., 2012). This also guarantees an excellent long-term stability of the optical signal.

Although the proposed biosensor is sensitive to surface RI changes that occur during the antibody/antigen interactions, a volume RI characterization is important for a complete investigation of the sensor performances. In order to characterize the device in terms of volume RI changes, six solutions at different RIs were prepared by mixing glycerol and water in various volumetric ratios, covering the range of refractive indices from 1.333 RIU of water up to 1.393 RIU of 40% glycerol-in-water solution, by following the protocol described in Supplementary materials.

The response of the sensor to changes in refractive index is detailed in Fig. S4, which shows the linear trend of the resonance wavelengths (λ_{RED}, λ_{BLUE} and $\Delta\lambda_{res}$) as a function of the refractive

index of the surrounding medium. By using a linear regression approach, it is possible to evaluate the volume RI sensitivity of the device k_{RI}, for all the resonant bands. The results are collected in Table 1.

TAP LPGs have been already demonstrated to attain values of volume RI sensitivity of the order of thousands nm RIU^{-1} (k_{RI}) (Tripathi et al., 2012; Garg et al., 2013). However, the results achieved here in terms of sensitivity (k_{RI} of 1309 nm RIU^{-1}) in the RI range of biological interest (i.e. 1.333–1.393 RIU) with a maximum error lower than 1% are particularly remarkable, since they were obtained using an LPG without any additional coating on the grating region.

3.3. Antibody/antigen model assay as biosensor performance evaluation

The effect of functionalization of the fiber surface using Eudragit L100 copolymer was initially explored. Fig. 2(a) shows the spectra before (gray) and after (black) Eudragit deposition, with the fiber surrounded by PBS. As it can be seen from the Figure, there are a blue-shift (i.e. decrease of λ_{res}) and a red-shift (i.e. increase of λ_{res}) of the resonant bands at the lower and higher wavelengths, respectively. In the enlargements (Fig. 2(b) and (c)), the experimental points are shown along with the fitting curves, drawn as solid lines. By using the procedure for data extraction detailed in Section 2.4, it is possible to achieve the value of both the resonance wavelengths (λ_{BLUE} and λ_{RED}) that characterize the dual resonant bands, as shown in the enlargements of Fig. 2(b) and (c), respectively. The vertical bars in the enlargements indicate the spectral position of the achieved resonance wavelengths.

By repeating three times the process of Eudragit deposition described in Section 2.3, a good repeatability was achieved: blue-shift of λ_{BLUE} equal to (2.7 ± 0.2) nm and red-shift of λ_{RED} equal to (2.9 ± 0.2) nm.

A real-time sensorgram during three injections of the antigen at different and increasing concentrations (1, 10 and 100 mg L^{-1}) is shown in Fig. 3. Each step is carried out following the same procedure: antigen injection with a flow rate of 25 μL min^{-1} for 15 min, washing phase with PBS buffer at a flow rate of 250 μL min^{-1} for 5 min and measurement phase stopping the flow for 5 min. These three phases are depicted in Fig. 3 with the letters A, B and C, respectively, in correspondence of the anti-IgG injection of 10 mg L^{-1}. The binding

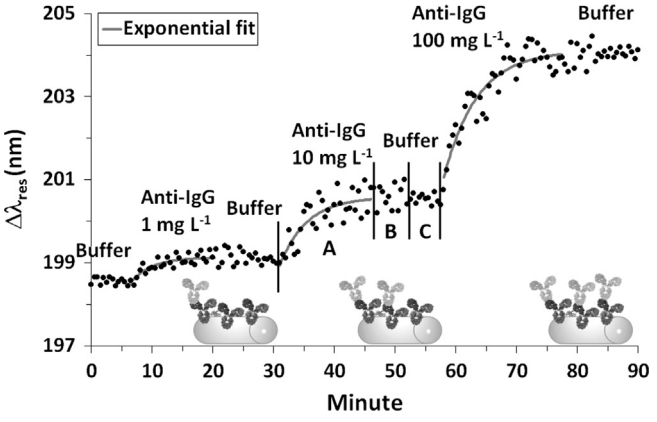

Fig. 3. Sensorgram during three antigen (anti-IgG) injections (1, 10 and 100 mg L^{-1}). The three regions A, B and C represent a complete measurement step. A: antigen injection (25 μL min^{-1}), binding time 15 min.; B: washing with PBS buffer (250 μL min^{-1}), washing time 5 min.; C: measurement in buffer (flow stopped), measurement time 5 min. The gray lines represent the exponential fitting curves for the binding regions.

Table 1
Volume RI characterization.

Parameter	λ_{RED}	λ_{BLUE}	$\Delta\lambda_{res}$
	Value and related uncertainty	Value and related uncertainty	Value and related uncertainty
Shift of λ_{res} (nm)	46.5 ± 0.3	-32.1 ± 0.3	78.6 ± 0.4
k_{RI} (nm RIU^{-1})	774.3 ± 4.1	-534.9 ± 4.3	1309.2 ± 5.9
Correlation	0.9997	0.9998	0.9999

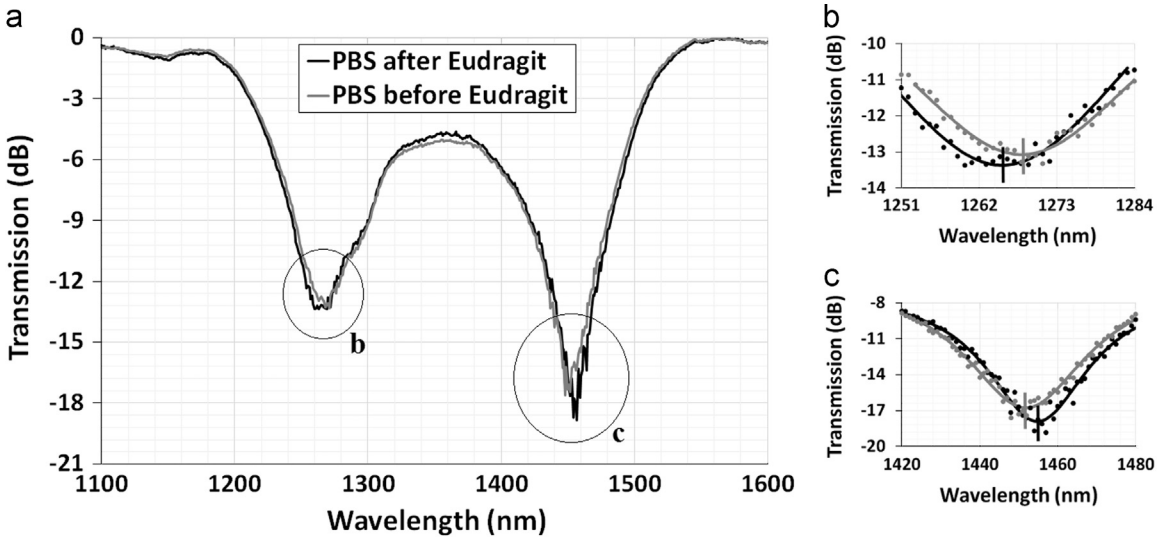

Fig. 2. (a) TAP LPG transmission spectra before (gray solid line) and after (black solid line) Eudragit L100 copolymer deposition. (b) and (c) enlargements of the peak regions: both the experimental points (gray, before Eudragit deposition, and black, after Eudragit deposition) and the fitting curves achieved with an ad-hoc developed NI–CVI® program are shown. The spectral position of the resonance wavelengths calculated with the program are indicated with vertical bars.

time of 15 min was the time needed to reach the saturation of the signal as also demonstrated by the exponential fit reported in Fig. 3. An increase of the $\Delta\lambda_{res}$ can be observed for the three concentrations, 1, 10 and 100 mg L^{-1}, with measured values of (199.2 ± 0.2) nm, (200.6 ± 0.2) nm and (204.1 ± 0.2) nm, respectively. As expected, the antibody–antigen interaction induces an increase of the signal and this effect can be explained considering an increase in both the thickness and the average RI of the deposited biolayer. The association profiles are highlighted by the single exponential fitting of the binding regions (gray lines): different association kinetics can be observed for the three concentrations with different curve slopes in the initial binding phase. The initial slopes of the fitting curves, which are 0.20 nm min^{-1}, 0.37 nm min^{-1} and 0.56 nm min^{-1} for antigen concentrations at 1 mg L^{-1}, 10 mg L^{-1}, and 100 mg L^{-1}, respectively, confirm the correlation between the initial rate of the binding reaction and the antigen concentration. The whole sensorgram (consisting of all the association and washing steps of all the tested concentrations) is not shown since the full measurement lasts a few hours but the long-term stability of the sensing system, already demonstrated (Trono et al., 2011), guarantees the absence of undesired drifts and/or fluctuations.

A first characterization of the proposed immunosensor was performed in PBS buffer exposing the TAP LPG to different concentrations of anti-mouse IgG (specific antigen), ranging from 1 μg L^{-1} to 100 mg L^{-1} and is shown in Fig. S5. The assay specificity was studied using anti-PSA at a concentration of 1 mg L^{-1}, following the same protocol used for the specific antigens. The shift of the $\Delta\lambda_{res}$ measured after the interaction with anti-PSA is (0.2 ± 0.2) nm, 6.5-fold lower than the shift of the $\Delta\lambda_{res}$ generated by the specific antigen at the same concentration.

A total wavelength shift (TWS) of 6.2 nm and a limit of detection (LOD), defined as three times the standard deviation of the blank, of 50 μg L^{-1} (330 pM) were achieved. This limit of detection is lower if compared with the results achieved with other LPG-based biosensors described in the literature (DeLisa et al., 2000; Deep et al., 2012; Tripathi et al., 2012; Chiavaioli et al., 2014), in which no additional coating except the biolayer is used. The comparison between the performance of the TAP LPG and a standard non-TAP LPG, performed with the same experimental setup on the same model assay (Chiavaioli et al., 2014), was carried out. Table 2 accounts for all the parameters of interest, starting from the statistical parameters up to the parameters extrapolated from the calibration curve. As it can be seen, TAP LPG shows better performance in terms of volume RI sensitivity, TWS and LOD. Anyway, it should be noted that, although the volume RI sensitivity increased of about a factor of 100, the TWS, evaluated into the same concentration range (Table 2), increased of about a factor of 30, confirming that the sensitivity of the LPGs as volume refractometer does not provide a realistic evaluation of the surface RI sensitivity.

As detailed in Table 2, the experimental standard deviation of the TAP LPG increased with respect to that one of a standard non-TAP LPG; this comes from the broadening of the spectral bandwidth, which implies a lower accuracy in the measurement of the resonant peak.

Table 2
Comparison of the results achieved with the TAP LPG and a standard non-TAP LPG.

Parameter	TAP LPG	standard non-TAP LPG (Chiavaioli et al., 2014)
Volume RI sensitivity (nm RIU^{-1})	1309	15
Maximum standard deviation (nm)	0.2	0.013
Maximum of residuals (nm)	0.2	0.012
Correlation	0.994	0.983
TWS (nm)	6.2	0.22
LOD (μg L^{-1})	50	500

It is worthy to be mentioned that only very preliminary results on biosensing in buffer samples with TAP LPGs are reported in the literature (Wang et al., 2009) and that the characterization in PBS of the proposed TAP LPG biosensor shows comparable or better performances with respect to the LPG-based biosensors in which a suitable overlayer was deposited over the grating region (Tang et al., 2006; Korposh et al., 2012; Yang et al., 2012; Pilla et al., 2012a).

The real effectiveness and feasibility of the proposed biosensor was assessed by performing the assay in human serum. Fig. 4 accounts for the calibration curve of the IgG/anti-IgG bioassay in human serum by drawing the differential shift of the two resonant bands $\Delta\lambda_{res}$ as a function of the concentration of each goat anti-mouse IgG (antigen) together with the logistic fitting curve. Each experimental point (squares) was obtained by averaging 15 distinct measurements after each washing step in PBS. The dashed black line indicates the value of $\Delta\lambda_{res}$ taken in PBS buffer before the injection of human serum.

Since the difference between the value of $\Delta\lambda_{res}$ in human serum and in PBS buffer is 0.2 nm (thus lower than the standard deviation), the specificity of the assay was effectively verified using human serum as real negative control. Based on the calibration curve performed in human serum, a TWS of 4.6 nm and a LOD of 70 μg L^{-1} were achieved in these conditions, thus demonstrating comparable performances of the LPG-based biosensor in buffer and in a complex matrix such as human serum.

4. Conclusion

A comprehensive study and a detailed analysis of a label-free optical immunosensor based on a turn-around point long period grating is discussed here for the first time, with only preliminary results being published in previous literature. Thanks to the use of a thermo-stabilized low-volume flow cell, which allows to carry out long-term measurements not affected by temperature and/or strain fluctuations/drifts, it was possible to achieve a full calibration curve of the bioassay both in buffer and in human serum.

By performing a comparison between the TAP LPG and a standard non-TAP LPG, we proved that the use of a higher cladding mode order (12th instead of 7th) implies not only an improvement of the sensor as a refractometer, which measures volume RI changes, but also an improvement of the sensor performance as biosensor.

Finally, in order to evaluate the real performance of LPG-based biosensors, the TAP LPG-based biosensor was characterized using

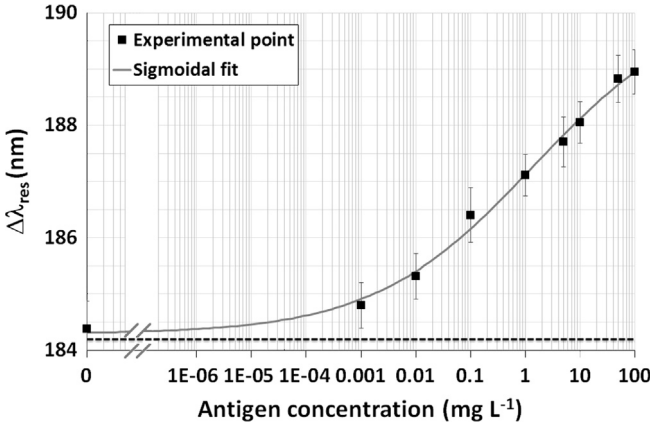

Fig. 4. Calibration curve of the bioassay performed with TAP LPG. Each experimental point (squares) is the average of 15 subsequent peak acquisitions. The black squares represent the exposure to different concentrations of anti-mouse IgG (specific antigen) in human serum, ranging from 1 μg L^{-1} to 100 mg L^{-1}. The solid gray line provides the best sigmoidal curve fitting of the experimental data, whereas the dashed black line represents the value of $\Delta\lambda_{res}$ taken in PBS before the injection of human serum.

human serum as complex matrix for the first time with respect to what proposed in the literature regarding LPG-based biosensors. Besides accomplishing the feasibility of the described model assay, with a LOD of 70 $\mu g\ L^{-1}$ (460 pM), the achieved results proved the goodness of the assay specificity.

Acknowledgments

The Authors are grateful for the financial support from the Joint Research Proposal (No. 22/EU/Italy/CNR/proj./2012) under CNR, Italy – CSIR, India Bilateral S&T Programme entitled "Development of Long Period Grating (LPG) based immunoassay for bio-sensing applications".

Appendix A. Supporting information

Supplementary data associated with this article can be found in the online version at http://dx.doi.org/10.1016/j.bios.2014.04.042.

References

Anemogiannis, E., Glytsis, E.N., Gaylord, T.K., 2003. J. Lightwave Technol. 21, 218–227.
Baldini, F., Brenci, M., Chiavaioli, F., Giannetti, A., Trono, C., 2012. Anal. Bioanal. Chem. 402, 109–116.
Chen, X., Zhou, K., Zhang, L., Bennion, I., 2007. Appl. Opt. 46, 451–455.
Chiavaioli, F., Trono, C., Giannetti, A., Brenci, M., Baldini, F., 2014. J. Biophotonics 7, 312–322.
Deep, A., Tiwari, U., Kumar, P., Mishra, V., Jain, S.C., Singh, N., Kapur, P., Bharadwaj, L. M., 2012. Biosens. Bioelectron. 33, 190–195.
Del Villar, I., Matías, I.R., Arregui, F.J., Lalanne, P., 2005. Opt. Express 13, 56–69.
DeLisa, M.P., Zhang, Z., Shiloach, M., Pilevar, S., Davis, C.C., Sirkis, J.S., Bentley, W.E., 2000. Anal. Chem. 72, 2895–2900.
Eftimov, T., 2010. Optical guided-wave chemical and biosensors II. In: Zourob, M., Lakhtakia, A., Wolfbeis, O.S. (Eds.), Springer Series on Chemical Sensors and Biosensors 8. Springer Berlin, Heidelberg, pp. 151–176.
Erdogan, T., 1997. J. Opt. Soc. Am. A 14, 1760–1773.
Estevez, M.C., Otte, M.A., Sepulveda, B., Lechuga, L.M., 2014. Anal. Chim. Acta 806, 55–73.
Fan, X., White, I.M., Shopova, S.I., Zhu, H., Suter, J.D., Sun, Y., 2008. Anal. Chim. Acta 620, 8–26.
Garg, R., Tripathi, S.M., Thyagarajan, K., Bock, W.J., 2013. Sens. Actuators B 176, 1121–1127.
Hill, K.O., Meltz, G., 1997. J. Lightwave Technol. 15, 1263–1276.
Homola, J., 2008. Chem. Rev. 108, 462–493.
Kindt, J.T., Bailey, R.C., 2013. Curr. Opinion Chem. Biol. 17, 818–826.
Korposh, S., Wang, T., Tatam, R., Lee, S.-W., 2012. Sens. Actuators B 173, 300–309.
Lepinay, S., Staff, A., Ianoul, A., Albert, J., 2014. Biosens. Bioelectron. 52, 337–344.
Patrick, H.J., Kersey, A.D., Bucholtz, F., 1998. J. Lightwave Technol. 16, 1606–1612.
Piliarik, M., Homola, J., 2009. Opt. Lett. 17, 16505–16517.
Pilla, P., Sandomenico, A., Malachovska, V., Borriello, A., Giordano, M., Cutolo, A., Ruvo, M., Cusano, A., 2012a. Biosens. Bioelectron. 31, 486–491.
Pilla, P., Trono, C., Baldini, F., Chiavaioli, F., Giordano, M., Cusano, A., 2012b. Opt. Lett. 37, 4152–4154.
Ramachandran, S., Wang, Z., Yan, M., 2002. Opt. Lett. 27, 698–700.
Shevchenko, Y., Francis, T.J., Blair, D.A.D., Walsh, R., DeRosa, M.C., Albert, J., 2011. Anal. Chem. 83, 7027–7034.
Shu, X., Zhang, L., Bennion, I., 2002. J. Lightwave Technol. 20, 255–266.
Tang, J.L., Cheng, S.F., Hsu, W.T., Chiang, T.Y., Chau, L.K., 2006. Sens. Actuators B 119, 105–109.
Tripathi, S.M., Bock, W.J., Mikulic, P., Chinnappan, R., Ng, A., Tolba, M., Zourob, M., 2012. Biosens. Bioelectron. 35, 308–312.
Trono, C., Baldini, F., Brenci, M., Chiavaioli, F., Mugnaini, M., 2011. Meas. Sci. Technol. 22 (075204), 9p.
Voisin, V., Pilate, J., Damman, P., Mégret, P., Caucheteur, C., 2014. Biosens. Bioelectron. 51, 249–254.
Wang, X.D., Wolfbeis, O.S., 2013. Anal. Chem. 85, 487–508.
Wang, Z., Heflin, J.R., Van Cott, K., Stolen, R.H., Ramachandran, S., Ghalmi, S., 2009. Sens. Actuators B 139, 618–623.
Yang, R.Z., Dong, W.F., Meng, X., Zhang, X.L., Sun, Y.L., Hao, Y.W., Guo, J.C., Zhang, W.Y., Yu, Y.S., Song, J.F., Qi, Z.M., Sun, H.B., 2012. Langmuir 28, 8814–8821.